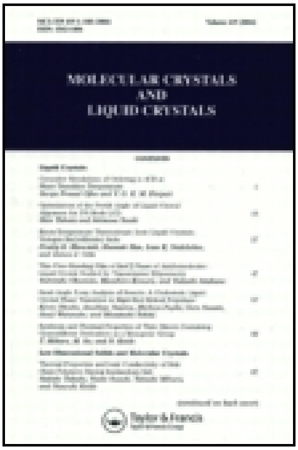

Molecular Crystals and Liquid Crystals

Publication details, including instructions for authors and subscription information:
http://www.tandfonline.com/loi/gmcl20

The Effect of Electric Fields on Selective Reflection in the SmC* Phase of Two Antiferroelectric Liquid Crystals

Upindranath Singh [a] & Helen Gleeson [b]

[a] Department of Physics, University of the West Indies, Bridgetown, Barbados

[b] Department of Physics and Astronomy, University of Manchester, Manchester, UK

Version of record first published: 31 Aug 2006

Mol. Cryst. Liq. Cryst., Vol. 439, pp. 125/[1991]–133/[1999], 2005

ISSN: 1542-1406 print/1563-5287 online
DOI: 10.1080/15421400590958098

The Effect of Electric Fields on Selective Reflection in the SmC* Phase of Two Antiferroelectric Liquid Crystals

Upindranath Singh
Department of Physics, University of the West Indies, Bridgetown, Barbados

Helen Gleeson
Department of Physics and Astronomy, University of Manchester, Manchester, UK

The effects of electric fields on the temperature dependence of optical Bragg reflections in the SmC phase of two chemically similar antiferroelectric liquid crystal were measured. These Bragg peaks are strong functions of temperature and applied fields resulted in Bragg peaks of reduced intensity and shifts to longer wavelengths. Relatively weak applied fields destroyed the Bragg peaks in both samples. The exact value of this applied field is strongly influenced by the magnitude of the dipole moment in each case.*

Keywords: antiferroelectric; Bragg scattering; electric-field effects; ferroelectric

INTRODUCTION

Chiral smectics, which exhibit ferro-, ferri- and antiferro-electricity, are currently the focus of intense research because of their great potential for applications in flat-panel displays [1–3]. Also, the rich polymorphism exhibited by these antiferroelectric liquid crystals make them attractive from the point of view of basic research. The ferroelectric (SmC^*) phase and the antiferroelectric (SmC_A^*) phase are the fundamental phases but additional intermediate phases have been identified [4]. In order to fully exploit the display potential of these materials, the electro-optic response of the various phases must be fully investigated. In this study, we focus on the temperature and field dependence of Bragg reflections in the SmC^* phase of two chemically similar heterocyclic esters.

Address correspondence to Upindranath Singh, Department of Physics, University of the West Indies, P.O. Box 64, Bridgetown, Barbados. E-mail: usingh@uwichill.edu.bb

In chiral smectic liquid crystals, chiral rod-like molecules are spontaneously tilted at a temperature-dependent angle (θ) with respect to the layer normal. In the SmC* phase, a macroscopic spontaneous polarization is observed in a direction normal to the tilt plane. Owing to the chirality of the molecules, the direction of the tilt and hence the spontaneous polarization slowly precesses around the layer normal as one moves along the direction perpendicular to the smectic planes. The period of this helical structure is typically hundreds of smectic layers and therefore represents a small chiral pertubation to the system.

The SmC_A^* phase is characterized by alternating layers which tilt in opposite directions. The spontaneous polarization also reverses in direction from one layer to the next. The neighbouring dipoles are nearly antiparallel and this results in very small value ($\approx$0) of the equilibrium electric polarization. Owing to its usually large dipole moment, strong coupling with external electric fields is expected in the SmC* phase but not the SmC_A^* phase. However, large enough fields will unwind the helix in both of these phases.

Bragg scattering is exhibited by all chiral liquid crystals whose helicoidal pitches are of the order of visible light. It has been used to study chiral nematic liquid crystals [5] and to identify phase transitions of the blue phases [6]. Bragg scattering is also a very sensitive probe for detecting transitions of chiral smectic liquid crystals whose pitches are comparable to visible wavelengths [7]. The helicoidal pitch in the intermediate or subphases are $\sim$1–2 μm and hence do not Bragg reflect visible light [8].

EXPERIMENT

The chemical structures of materials studied are shown in Figure 1. These materials were purchased from Kingston Chemicals.

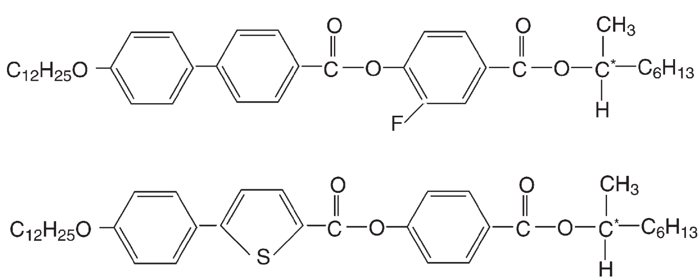

FIGURE 1 Chemical structures of the materials studied (top AS661: bottom AS612).

There is still considerable debate with regard to the phase transitions of AS661 since different techniques have yielded different sequences for this material [9–13]. However, the following phases have been identified [11] for AS661 and this is consistent with our optical activity data [9].

$$SmC_A^* \xrightarrow{77.9} FI1 \xrightarrow{80.3} FI2 \xrightarrow{84} AFE \xrightarrow{88.2} SmC_\beta^* \xrightarrow{94} SmA \xrightarrow{106} I$$

SmC_β^* is a ferroelectric phase and all temperatures are in °C. AS661 has also been referred to as 12OF1M7 and 12FM17 [12,13].

The phase sequence of AS612 (which has been less studied than AS661) is [14]:

$$SmC_A^* \xrightarrow{80.2} FI1 \xrightarrow{82.2} SmC^* \xrightarrow{92.6} SmA \xrightarrow{97.9} I$$

The apparatus for detecting optical Bragg peaks has been described in detail elsewhere so only an outline of the technique is given here [7]. The samples were placed on the hot stage of a reflecting polarizing microscope, heated to the desired temperature and allowed to equilibrate. The light reflected from the sample was diverted into an Optilas Chromex 250 scanning monochromator (accurate to ±0.05 nm) and then onto a photomultiplier tube. A Linkam hot stage (TMS600) and temperature controller (TMS93) combination provided temperature control to ±0.1 K. The samples were contained in commercially available 50 µm thick ITO coated cells, which were treated for homeotropic alignment to ensure correct orientation of the helix axis. The electrode pattern provided an in-plane field that acted normal to the helical axis.

RESULTS AND DISCUSSION

The SmC^* phase of both samples selectively reflect visible light (see Fig. 2). Also, the greatest change in pitch occurs over a one-degree temperature interval just below the SmA–SmC^* transition and each reflection spectrum contains a broad maximum. The SmC^* phase is stable over 7.4 K in AS661 and 10.2 K in AS612. These temperature intervals are consistent with those of references 9 and 11. These ranges are easily determined since the SmC^* is sandwiched between two non-reflecting phases in these materials [7]. In some materials (but not in our case) it may be difficult to pinpoint the SmA–SmC^* transition, if the relevant Bragg peaks are in the UV region. For the SmC_A^* phase, Bragg peaks in the visible region can be detected for AS661 but not for AS612. The Bragg peaks observed in the SmC_A^*

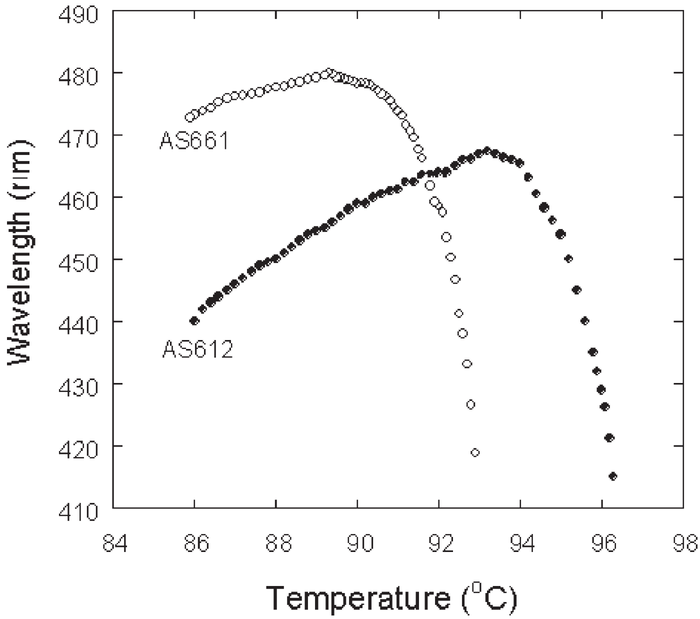

FIGURE 2 Bragg wavelengths selectively reflected by the SmC* phase of AS661 (○) and AS612 (●).

phase of AS661 are slightly longer than those for the corresponding SmC* phase [7].

Both full pitch [15–17] and half-pitch [18] reflections have been reported for Bragg scattering in the SmC* phase. Shtykov, Vij and Nguyen [16] published microphotographs of homeotropic textures of 11OTBBB1M7. Bright uniform colours were observed for both the SmC^*_A (red) and SmC* (green) phases. They attributed that the wavelengths selectively reflected are related to the full pitch in the SmC* phase and to the half pitch in the SmC^*_A phase.

To determine if the observed reflections are due to full pitch or half pitch bands we observed the light emanating from slightly inclined homeotropic samples. Half pitch reflections are visible only along the helical axis. Full pitch bands are observed from the side and a continuous shift in wavelengths is observed as the viewing angle is changed. Based on these observations we deduce that we have observed full pitch reflections in AS612 and half pitch reflections in AS661. Also, half pitch reflections can be established using the light diffraction technique of Kondo *et al*. [18]. Unfortunately, we are not equipped to carry out such experiments at this time.

The critical field for the unwinding of the helix by an a.c. field is given by [19]:

$$E_c = \frac{\pi^2}{p_0}(8\pi^2 K/\varepsilon_a)^{0.5} \tag{1}$$

where p_0 is the undisturbed helical pitch, K the elastic and ε_a is the dielectric anisotropy. If we ignore the temperature dependence of K and ε_a, then E_c is proportional to $p_0(T)$. Since the Bragg reflections (Fig. 2) each contain a broad maximum then one would expect a broad minimum for the temperature dependence of the critical voltages. This is indeed what is observed (Fig. 3).

It is useful to report a few general trends prior to discussing the effects of electric fields on each material in detail. The fields were applied in the plane of the smectic layers (normal to the helical axis). The coupling between the external field and the spontaneous polarization distorts the helix. As the external field is increased, more and

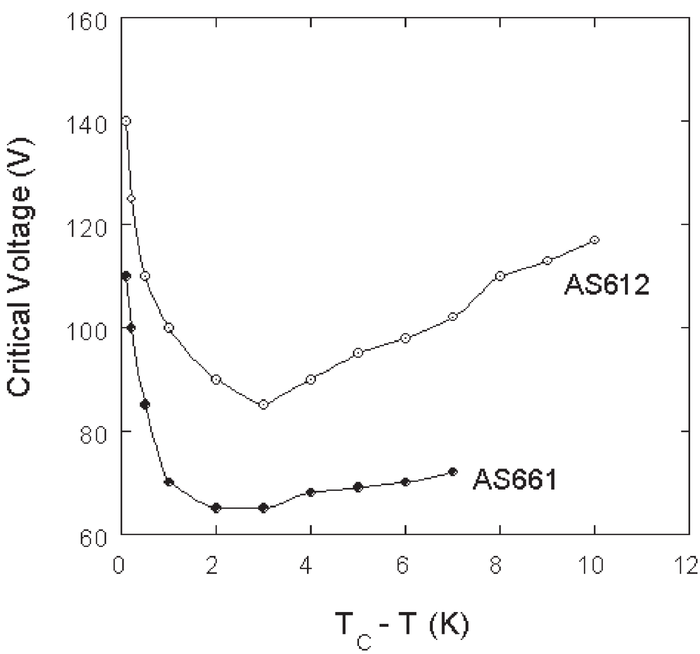

FIGURE 3 Temperature dependence of the critical voltage (23 Hz, A.C.) required to unwind the helix in the SmC* phase of the materials studied. Each cell has an electrode gap of 1 mm and a sample thickness of 50 μm. The lines are merely guides to the eyes.

more molecules are aligned in a plane perpendicular to the field direction, until at a critical electric field, the structure unwinds and we obtain a homogeneous, uniformly polarized tilted smectic phase.

For each sample, the temperature dependence of the critical voltage (see Fig. 3) contains a broad minimum at temperatures $\sim$2–3 K below the SmA–SmC* transition (T_C). Relatively small fields $\sim 10^5$ V/m are sufficient to completely unwind the helix in both AS661 and AS612. In general, the critical field for AS661 is smaller than that in AS612 at the same reduced temperature ($T_C - T$). The saturation values of the polarization of both materials have been previously reported [14]. They are 125 nC/cm^2 and 105 nC/cm^2 for AS612 and AS661 respectively. Based on these values one would expect the critical field for AS661 to be higher than that of AS612. However, the higher value of the critical voltage for AS612 is most likely due to the shorter pitch of this material, suggesting that the measured reflections in AS612 are consistent with full pitch bands.

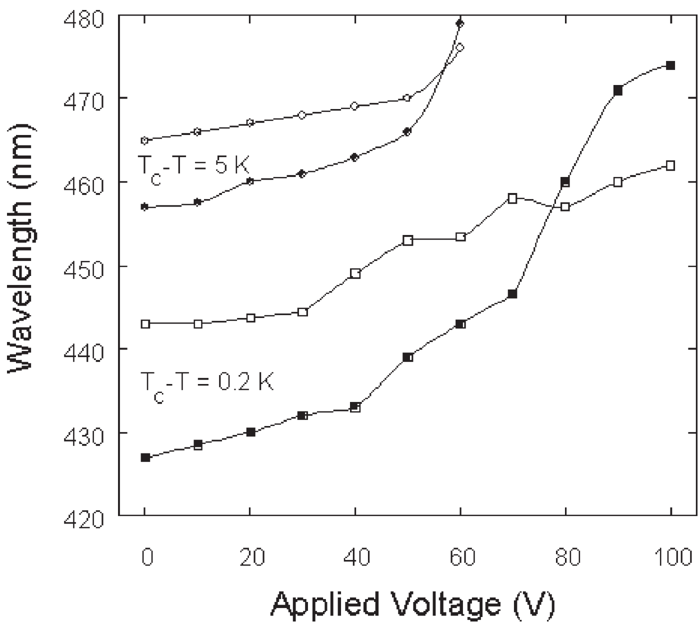

FIGURE 4 The variation of Bragg wavelengths with applied voltages at two different temperatures in the SmC* phase of AS661. Solid symbols correspond to increasing voltages while decreasing voltages are represented by open symbols. The lines are merely guides to the eyes.

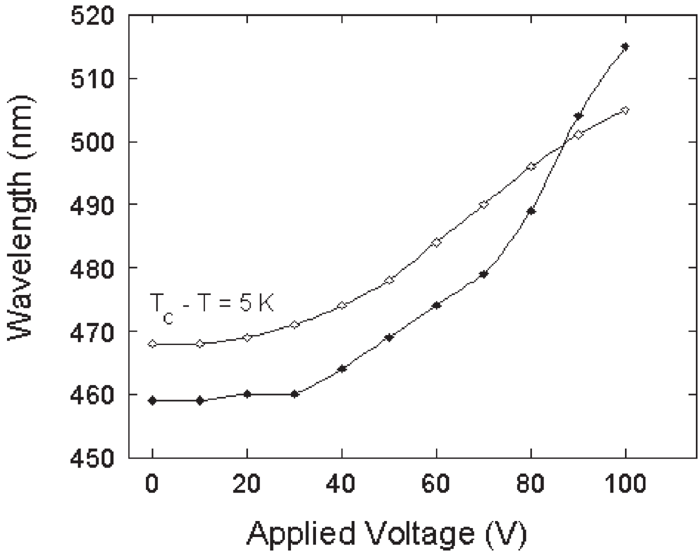

FIGURE 5 The variation of Bragg wavelengths with applied voltages in the SmC* phase of AS612. Solid symbols correspond to increasing voltages while decreasing voltages are represented by open symbols. The lines are merely guides to the eyes.

For a given temperature, if an applied field is strong enough to produce a measurable wavelength shift but not strong enough to unwind the helix in the SmC* phase, then there is little or no hysteresis in the Bragg peaks when this field is reduced to zero. However, if an applied field is strong enough so as to completely unwind the helix (Bragg reflections disappear), hysteresis is observed. At all temperatures studied, the pitch increased as the magnitude of the voltage increased. Also, the corresponding Bragg signals became weaker and more and more asymmetric.

The shifts in the Bragg peaks with increasing and decreasing voltages are shown in Figures 4 and 5 for AS661 and AS612 respectively. The curves corresponding to the different temperatures are similar in topology in both materials. For all temperatures studied, the curves corresponding to increasing and decreasing voltages, intersected at voltages close to the critical voltages. Also, the zero-field Bragg wavelengths and thus, the corresponding pitches increased after the helix was destroyed and then allowed to reform. This might be relevant to display devices.

It has been shown that the helical period diverges at the critical field [19,20]. This divergence though not so obvious at temperatures just below the SmA–SmC* transition where the helix might not be fully formed is evident in both samples at lower reduced temperatures. The unwinding of the helix in the SmC* phase of a ferroelectric liquid crystal does not increase continuously, but rather shows discontinuous jumps, each corresponding to the exclusion of a single 2π domain from the sample [20]. This situation may also exist in antiferroelectric liquid crystals [20] and the different slopes in our data could be due to the step-by-step unwinding of the helix in the SmC* phase of AS661 and AS612.

Linear regions are evident in the electro-optic response of the samples in both the unwinding and rewinding stages. The curve corresponding to increasing voltages (solid symbols in Fig. 4) for AS661 at a temperature $T_C - T = 0.2\,K$ contains three linear regions. The slopes of these linear regions increase with increasing applied fields. This means that it becomes progressively easier for the helix to be stretched once the process has begun. Linear regions are also evident in Figure 5 for AS612. The linear regions in Figures 4 and 5 also suggest that the helix also forms in a step-by-step fashion.

CONCLUSION

This study has provided detailed information on the temperature and field dependence of optical Bragg reflections in the SmC* phase of two chemically similar antiferroelectric liquid crystals. The pitches in these materials follow a nonlinear temperature dependence with the greatest change in pitch occurring within $\sim$1 K below the SmA–SmC* transition. In all cases, the pitches increased as the magnitude of the applied voltage increased. There is considerable hysteresis in the Bragg peaks if the helix is unwound and then allowed to reform by reducing the applied voltage but little hysteresis if the helix is not first unwound. Despite its larger saturation polarization, the critical voltage for AS612 its higher than that of AS661. This is probably due to a shorter helical pitch in AS612.

REFERENCES

[1] Clark, N. A. & Lagerwall, S. T. (1980). *Appl. Phys. Lett.*, *36*, 899.
[2] Yamada, Y., Yamamoto, K., Nakamura, K., Kawamura, I., Hagiwara, T., & Suzuki, Y. (1995). *Proc. 5th Int. Conf. Ferroelectric Liquid Crystals*, T52.
[3] Yamamoto, N., Koshoubu, N., Mori, K., Nakamura, K., & Yamada, Y. (1993). *Ferroelectrics*, *149*, 295.
[4] Fukada, A., Terashima, K., Ichikawa, K., & Takezoe, H. (1994). *Ferroelectrics*, *4*, 997.
[5] Gleeson, H. F. & Coles, H. J. (1989). *Mol. Cryst. Liq. Cryst.*, *170*, 9.

[6] Nicastro, A. J. & Keyes, P. H. (1983). *Phys. Rev. A.*, *27*, 431.
[7] Singh, U., Gleeson, H., Goodby, J., & Hird, M. (2002). *Ferroelectrics*, *277*, 153.
[8] Matkin, L. S., Gleeson, H. F., & Watson, S. (2001). *Phys. Rev. E.*, *64*, 021705.
[9] Singh, U., Harris, O., & Hunte, C. (2002). *Liq. Cryst.*, *31*(6), 853.
[10] Robinson, W. K. (1995). Ph.D. thesis, University of Manchester, UK.
[11] Baylis, L. J., Gleeson, H. F., Seed, A. J., Styring, P. J., Hird, M., & Goodby, J. W. (1999). *Mol. Cryst. Liq. Cryst.*, *328*, 13.
[12] Shtykov, N. M., Vij, J. K., Lewis, R. A., Hird, M., & Goodby, J. W. (2000). *Phys. Rev. E.*, *62*, 2279.
[13] Fera, A., Opitz, R., de Jeu, W. H., Ostrovskii, B. I., Schlauf, D., & Bahr, Ch. (2001). *Phys. Rev. E.*, *64*, 021702.
[14] Watson, S. J., Matkin, L. S., Baylis, L. J., Bowring, N., Gleeson, H. F., Hird, M., & Goodby, J. W. (2002). *Phys. Rev. E.*, *65*, 031705.
[15] Kondo, K., Fukuda, A., & Kuze, E. (1981). *Jpn. J. Appl. Phys.*, *20*, 1779.
[16] Shtykov, N. M., Vij, J. K., & Nguyen, H. T. (2001). *Phys. Rev. E.*, *63*, 051708.
[17] Akizuki, K., Miachi, K., Takanshi, Y., Ishikawa, K., Takezoe, H., & Fukada, A. (1999). *Jpn. J. Appl. Phys.*, *38*, 4832.
[18] Kondo, K., Takezoe, H., Fukuda, A., & Kuze, E. (1982). *Jpn. J. Appl. Phys.*, *21*, 1779.
[19] Wang, Z. H., Sun, Z. M., & Feng, D. (1991). *Europhys. Lett.*, *14*(8), 785.
[20] Conradi, M., Kityk, A. V., Škarbot, M., Blinc, R., & Muševis, I. (1999). *Liq. Cryst.*, *26*(8), 1179.